Quantum Dot Sizes from their Spectra

- Lab Practice - Physics at the Nanoscale UAB -

Valentina Ayala Calixto, Daniel Bedmar Romero ,
Astrid Mayné Arévalo , Xabier Oyanguren Asua

Abstract— Employing the infinite and finite potential energy well quantum models, we characterise the particle sizes and dispersions of different cadmium selenide CdSe quantum dot (QD) samples, based only on their emission spectra.

1 Introduction

Semiconducting nanoparticle (NP) solutions show an enhanced absorption and emission spectra at room temperature when compared with the bulk material. This is because the confinement of the excitonic states increases their binding energy, stabilizing excited states, while the transition rates become inversely proportional to the NP diameter [1].

The smaller the QD, the bigger the band gap will be, due to the decreased number of atoms forming the band structure. This implies more energetic photons will be necessary to excite the electrons in the valence band (VB) and more energetic light will be emitted in turn [1]. Then, by using the right physical model, it should be possible to determine the sizes of the NPs in a problem solution, by simply analysing their spectral profile, as a cheaper alternative to other characterisation techniques like microscopy.

2 Experimental Procedure

We were given 6 problem samples (see Figure 1), each with an unknown dispersion of polymer coated cadmium selenide (CdSe) QDs. We irradiated each of the samples with the same UV light source and then guided, with the use of an optical fiber, the output light from a partially occluded position relative to the UV lamp (to avoid saturation) to an Avaspec 2048 spectrophotometer. The device then digitalized the measurement of the spectral emission profiles. See in Figure 2 the measured spectra for each sample, as labelled in Figure 1.

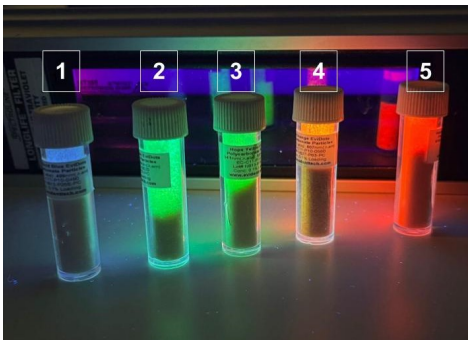

Figure 1: Five of the six problem samples that were given to analyse, when illuminated with the UV lamp. The sample we label as 6-th (with a colour in between samples 2 and 3) was enclosed in a chamber to allow a proper measurement of its dimmer emission.

Note that we do not need to know the wavelength of the UV source, as long as it is able to excite the electrons of the QDs to their VBs. This is because we assume electrons will decay non-radiatively until the bottom of the VB and to the most stable excitonic state, from where the radiative transition of the characteristic wavelength of the QD will occur.

We see in Figure 2 that all samples (except number 6, which had a cage to extract the emission of the QDs alone), have a common background at small and big wavelengths, which are due to the ambient light and the UV lamp itself. The part of the spectrum that changes from sample to sample lies in the visible light range in all cases, without complete overlap with the UV lamp's wavelengths. Then, in order to isolate the excitonic emission we could subtract an average background to the spectra, yet, the background notably varies between samples (since it had to do with the manual position in which the optic fibre was placed). Therefore, we decided to isolate the excitonic emission peaks by manually selecting an adequate window around them avoiding interference with the background. The selected windows can be seen in Figure 2.

The emission peaks, which move in wavelengths due to the variation of the QD sizes from sample to sample, have an approximately Gaussian shape in all cases, suggesting that the QDs have a continuous size range with a Gaussian distribution, with a different main particle diameter and dispersion per sample. We can say so instead of attributing the width of the peak to Heisenberg's uncertainty principle for a single QD size per sample, because excitonic transition times are known to be in the order of $1ps$ [2], which would only give a dispersion in wavelength on the order of $1pm$ or $0.001eV$, smaller than the the observed widths of the profiles.

3 Theoretical Procedure

3.1 General Algorithm

In order to study the emission profiles given by a distribution of QDs of different sizes, due to the superposition principle of Maxwell's Equations, we may assume that the total intensity of the spectrum is the sum of the contributions of each QD present in the solution.[1] Then, in general, given an arbitrary density function $\rho(R)$ for QDs in a solution, as a function of their radius R, assuming a QD of radius R has an emission spectrum $F(R, E)$ as a function of the energy E, the total emission spectrum I will be given by the continuous weighted sum [3]:

$$I(E) = \int_{-\infty}^{\infty} \rho(R)F(R, E)\, dR \tag{1}$$

Then, following the observations of the previous section we can assume the size distribution of the QDs $\rho(R)$ follows a gaussian distribution:

$$\rho(R) = \frac{N}{\sigma_R\sqrt{2\pi}} e^{-\frac{(R-R_0)^2}{2\sigma_R^2}} \tag{2}$$

where R_0 is the mean radius of the QDs of the solution and σ_R their size standard deviation, indicating the size dispersion. The computation of these two parameters for each of the problem samples is the objective of the present work.

We assume that the emission spectrum of a QD of size R has a Gaussian shape centered in its lower excitonic level energy (relative to the VB) $E_e(R)$:

$$F(R, E) = \frac{\alpha(R)}{\Gamma\sqrt{2\pi}} e^{-\frac{(E-E_e(R))^2}{2\Gamma^2}} \tag{3}$$

[1] Note that we assume then that there is no quenching or similar effect between QDs of the same solution.

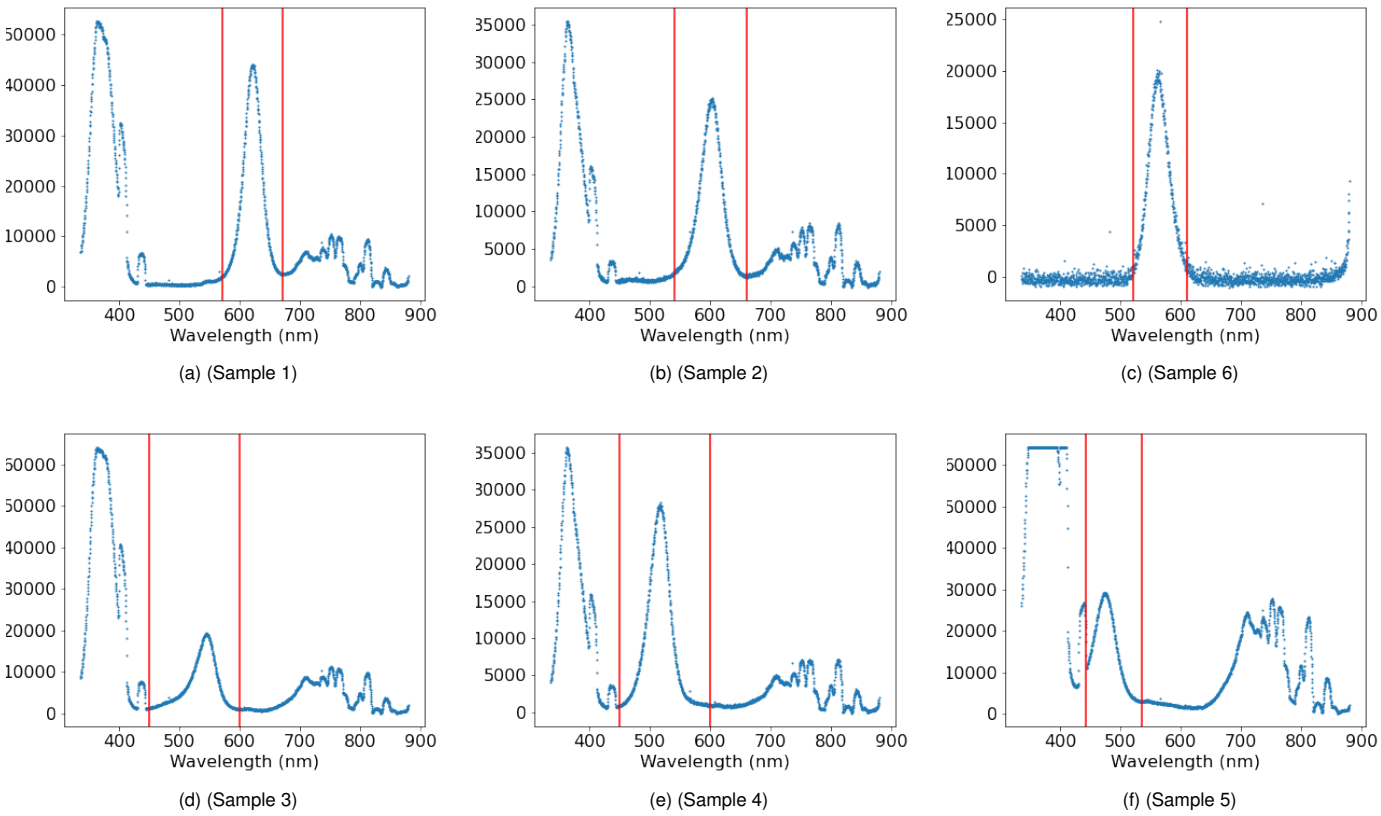

Figure 2: Measured spectra of the 6 samples with the windows selecting the excitonic contribution marked with red vertical lines. The y axes indicates the emission intensity counts in arbitrary units.

where Γ is the standard deviation of the emission for a single QD, while $\alpha(R)$ is the emission efficiency of the QD as a function of R. We will use as the intrinsic coefficient Γ the Heisenberg estimate we calculated above $\simeq 0.01eV$. On the other hand, the coefficients $\alpha(R)$ could be estimated as being proportional to the excitonic absorption rate, obtained using Fermi's golden rule [1], or by some empirical law under Beer-Lambert law calibrations [4]. However, for the sake of simplicity, we will assume that for any given problem sample, the dispersions σ_R will be small enough as to make the variation of $\alpha(R)$ negligible. Thus, we will assume $M := N\alpha$ to be a certain normalisation constant for the emission profile $I(E)$.

Then, assuming that we have a physical model giving an analytic or numerical shape for $E_e(R)$, we have that the predicted emission spectrum will be parametrized by only three unknown variables: the normalization constant M, the average size R_0 and the dispersion σ_R, forming the theoretical prediction $I(E; M, R_0, \sigma_R)$. Then, given we have a set of observed pairs of values $\{(E_j,\ \hat{I}_j)\}_{j=1}^n$ (the ones plotted in Figure 2), we can find the best fitting parameters M, R_0, σ_R, for a given sample, with which we will predict R_0 and σ_R.

For this we will consider a cost function C

$$C(M, R_0, \sigma_R) = \sum_{j=1}^{n} (I(E_j;\ M, R_0, \sigma_R) - \hat{I}_j)^2, \qquad (4)$$

that will be minimized by a non-linear optimizer, to give the best-fitting R_0, σ_R (through the best-fitting theoretical $I(E)$ profile).

3.2 Energy-QD size relations

The question then is translated into finding an expression or numerical estimation for the transition energies from VB to the excitonic level, $E_c(R)$, as a function of the QD radious R. For this, we can model the CdSe nanoparticle as a bulk crystal lattice that gets confined inside a spherical potential energy well of a size equal to the diameter of the QD. There, the electron-hole pair forming the exciton is treated as a semiclassical quasi-free carrier pair through their effective masses [1]. Because CdSe excitons are seen to have a bulk Bohr radius on the order of $50\mathring{A}$ [1], it will be important not to treat the excitons as free particles within the crystal (with an energy contribution in analogy with the free Hydrogen atom), but as a confined pair of particles (since in fact it is this what allows them to have so efficient emission spectra [1]). This is justified because we will find QD sizes in the order of nm. It is the so called strong-confinement regime.

3.2.1 *Assuming Infinite Wall Spherical Energy Well*

Assuming the strong-confinement walls are modelable as impenetrable barriers, Ref. [5] developed the following analytic expression for the first order perturbative estimate of the exciton energy

$$E_e(R) \simeq E_{bulk}^{gap} + \frac{\hbar^2\pi^2}{2\mu R^2} - 1.786\frac{e^2}{\varepsilon_S R} + \beta\frac{e^2}{\varepsilon_s R}, \qquad (5)$$

where $\beta := -2\sum_{n=0}^{\infty} \frac{(\varepsilon-1)(n+1)}{(n\varepsilon+n+1)} \int_0^1 x^{2n} sin^2(\pi x) dx$; $\mu := (1/m_e + 1/m_h)^{-1}$ is the reduced mass with m_e, m_h the effective masses of the electron and hole in the bulk material, e is the charge of the electron and ε_S is the permittivity of the bulk material.

The first term accounts for the band-structure sustaining the exciton. The second one is due to the confinement of the electron and hole in a sphere of radius R (it is the lowest eigenenergy of the infinite spherical well for an otherwise uninteracting electron-hole pair). The third term is the first order perturbative energy correction accounting for the Coulomb interaction of the localised and overlapping electron and hole wavefunctions. Last but not least, the fourth term accounts for the surface polarization of the sphere (the interface with the shell). In particular, due to the complicated shape of the polarization term and because Ref. [5] shows that for CdSe QDs with a radius in the order of nm the polarization term is one third of the Coulomb term (with opposed sign), we will only add this correction, just as done by Ref. [3].

3.2.2 Assuming Finite Wall Spherical Energy Well

When the confinement is very strong, meaning that the QD radius R is made very small, the infinite potential well picture may become unsatisfactory. This is because the polymer coating the CdSe core supposes a finite energy barrier for the exciton, given by the energy difference of their conduction bands. In particular, we are told that the barrier in our problem samples has 4 eV. Then, it is important to allow the penetration of the exciton to the coating layer in the physical model, because among others, it is well known that a finite spherical well is not forced to have a bound state if R is small enough (while in the infinite case there is always at least a bound state within the well).

In order to model a finite well containing the Coulomb interacting electron-hole pair (in particular, we only need to know the gap energy as a function of the particle radius $E_c(R)$), several methods are used in the literature, mainly centred on variational approaches like Ref. [6]. These provide a computationally expensive ad-hoc approach for each problem at hands, so we could not follow them. An alternative could be to employ empirically fitted curves like the ones provided by Ref. [4].

Instead, as a first approximation, we thought on the following. With the same idea as in the previous section, but applied to a finite well, we could set:

$$E_e(R) \simeq E_{bulk}^{gap} + \sum_{j\in\{h,e\}} E_{sph}^{fin}(R,\ m_j) - 1.786\frac{e^2}{\varepsilon_S \tilde{R}} + \beta\frac{e^2}{\varepsilon_s \tilde{R}}, \tag{6}$$

On the one hand, $E_{sph}^{fin}(R,\ m_j)$ is the ground state energy for the finite spherical well with a particle of mass m. This energy follows the same transcendental equation as for the odd parity confined states in the 1D finite well:

$$2\sqrt{E(V_0 - E)} - (V_0 - 2E)\, cotan(\frac{\sqrt{2mEd^2}}{\hbar}) = 0 \tag{7}$$

which can be numerically obtained for each R. On the other hand, we substitute R by $\tilde{R} := R + \delta$, instead of calculating the new perturbative Coulomb interaction and polarization terms. This is legitimate because in a first order approximation, if the core of the probability density is within the well (as is the case in QDs), the finite well ground-state can be approximated as the one for the infinite well but extending to a radial distance $\tilde{R} := R+\delta$ instead of R. This δ would be the penetration distance (the exponential decay factor) of the wavefunction in the shell, which is known to be given by $\sqrt{2m(V_0 - E)}/\hbar$.

Fortunately, we found Ref. [7], who gives an analytical formula for $E_e(R)$ in a finite well, by generalising Eq. (8) to finite potentials (in a first order perturbative fashion). For this, they use an analytic shape for the trascendental energy equation (with a Bessel function) to then derive analytic perturbative terms using as ansatz for the electron and hole wavefunctions, the ground-state Hydrogen orbitals. All in all, neglecting the interface polarization term, they get that,

$$E_e(R) \simeq E_{bulk}^{gap} + \sum_{j\in\{h,e\}} \frac{\hbar^2\pi^2}{2m_j R^2} f(\nu_i)^2 + E_{e-h}(R), \tag{8}$$

where

$$f(\nu_i) := \left(1 + \frac{1}{\nu_e} + \frac{(\pi/2-1)^2}{\nu_e(\nu_e - 1)}\right)^{-1}$$

and

$$E_{e-h}(R) := -\frac{e^2}{\varepsilon_s R}\left(\frac{2\pi^{-5/2} f(v_h)^{-1} f(v_e)^{-3/2}}{j_1[\pi f(\nu_e)] j_1[\pi f(\nu_h]}\right)^2 \Big\{-\frac{1}{4}Si[2\pi f(\nu_e)] -$$

$$-\frac{1}{8}Si[2\pi(f(\nu_h) - f(\nu_e))] + \frac{1}{8}Si[2\pi(f(\nu_h) + f(\nu_e))] +$$

$$+\frac{f(\nu_e)}{2f(\nu_h)}[\pi f(\nu_h) - cos(\pi f(\nu_h)) sin(\pi f(\nu_h))]\Big\}.$$

Such that, $\nu_i := (2V_0 m_i R^2/\hbar^2)^{1/2}$, $j_1(x)$ is the first-order spherical Bessel function, and $Si[x] := \int_0^x \frac{sin(t)}{t} dt$.

4 Results and Discussion

Employing a Python script, we parse the digitalised spectrum of each sample and run over them the algorithm presented in the previous section (the non-linear optimization is performed using the Nelder-Mead algorithm in the *scipy* library [8]). The best fit curves obtained after fixing adequate initial conditions for the optimizer, with 2000 iterations till best convergence, can be found in Figure 3 for the infinite potential well and in Figure 4 for the finite potential case. The script is left as open source in the Github page of the practice [9]. The employed constants for $CdSe$ were $\varepsilon_S = 4\pi 8.3\varepsilon_0$ with ε_0 the perimittivity of vacum, $E_{bulk}^{gap} = 1.8eV$, $m_e = 0.13m$ and $m_h = 0.45m$, with m the rest mass of the electron [1].

In Table 1, the predicted mean size and dispersion for the QDs in each sample can be found, computed using either the finite and infinite potential models.

We see in Table 1, that the estimates given by the finite potential model for the mean radii R_0 are smaller than the infinite potential ones, while the standard deviations are predicted to be bigger. This last observation suggests that the finite potential well model has a higher sensitivity regarding the dispersion of sizes. What is interesting though is that the emission energy E_{exc} predicted for either the mean radii R_0 or a range of width σ_R around it, are roughly equal for the optima of both models (exactly equal regarding the first two rounded decimal places in all but Sample 2). This should nevertheless be readily expected if the fitting power of both models is the same. That is, it is expectable that the fitted peaks of the emission profiles will land in the same energies for an optimal fit with the experimental data. This is especially obvious if we notice that both models show the same functional dependence for the energy as a function of the radius, except for multiplicative constants (they are both a constant term plus a term proportional to the inverse of the radius squared, plus a term proportional to the inverse of the radius).

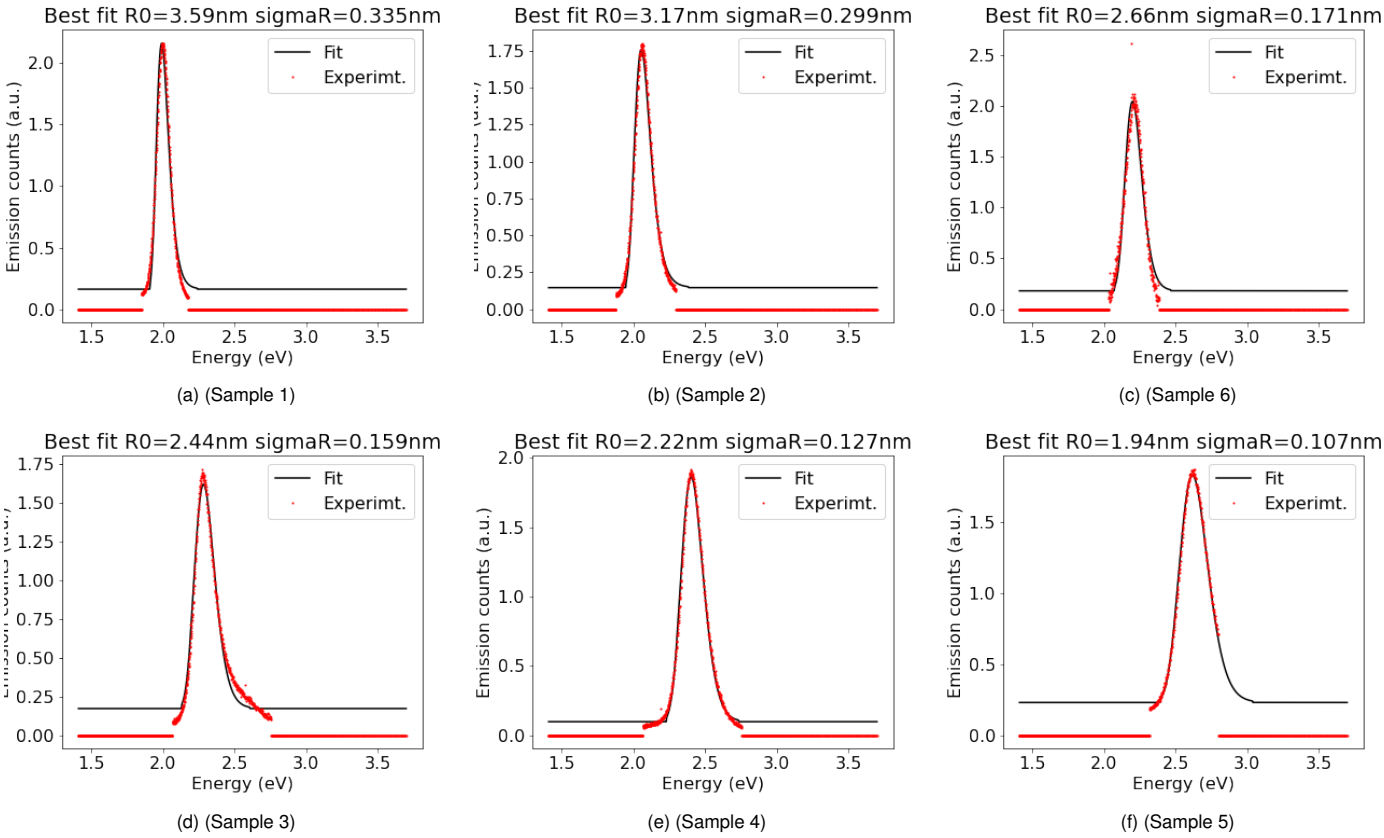

(a) (Sample 1) (b) (Sample 2) (c) (Sample 6)

(d) (Sample 3) (e) (Sample 4) (f) (Sample 5)

Figure 3: Selected experimental data in red and theoretical fit using the infinite quantum potential well model in black.

Table 1: Calculated parameters for the 6 samples with both infinite and finite quantum well models. $E_{exc}(R_0)$ stands for the excitonic emission energy at the predicted average radius R_0, while $E_{exc}\ range$ is the predicted energy range for $R \in (R_0 - \sigma_R, R_0 + \sigma_R)$, giving an impression of the dispersion in energy space.

	Infinite Potential				**Finite Potential**			
Fitted Parameters	$R_0(nm)$	$\sigma_R(nm)$	$E_{exc}(R_0)(eV)$	E_{exc} *range*	$R_0(nm)$	$\sigma_R(nm)$	$E_{exc}(R_0)(eV)$	E_{exc} *range*
Sample 1	3.59	0.335	2.0	(1.96, 2.06)	3.39	0.344	2.0	(1.96, 2.06)
Sample 2	3.17	0.299	2.07	(2.02, 2.14)	2.94	0.351	2.08	(2.02, 2.16)
Sample 6	2.66	0.171	2.21	(2.16, 2.28)	2.44	0.176	2.21	(2.16, 2.28)
Sample 3	2.44	0.159	2.3	(2.23, 2.38)	2.22	0.164	2.3	(2.23, 2.38)
Sample 4	2.22	0.127	2.42	(2.34, 2.5)	1.99	0.131	2.42	(2.34, 2.5)
Sample 5	1.94	0.107	2.63	(2.54, 2.74)	1.69	0.111	2.63	(2.54, 2.74)

Comparing with the reference [10], we can see that the values obtained do not differ much from those that were obtained (in a range of 23 to 55 Å) for spectrum wavelengths λ in $(475, 650)$ nm.

5 Conclusions

We have proved that fitting a simple theoretical model to the emission spectrum of a sample containing a Gaussian dispersion of QDs allows a quantitative determination of their sizes. This is a very low-cost method that may be employed instead of the more expensive alternatives, such as microscopy. We have also proved that by using more accurate models (the finite potential well instead of the infinite one, for example), the predictions get quantitatively more sensitive. It is left as future work to check the agreement of the predictions with size and dispersion estimations made with alternative techniques, and to check if improved versions of the models (like including the polarization terms), make more accurate predictions.

References

[1] J. H. Davies, *The physics of low-dimensional semiconductors: an introduction*. Cambridge university press, 1998.

[2] C. de Mello Donegá, M. Bode, and A. Meijerink, "Size- and temperature-dependence of exciton lifetimes in cdse quantum dots," *Phys. Rev. B*, vol. 74, p. 085320, Aug 2006.

[3] T. Ravindran, A. K. Arora, B. Balamurugan, and B. Mehta, "Inhomogeneous broadening in the photoluminescence spectrum of cds nanoparticles," *Nanostructured materials*, vol. 11, no. 5, pp. 603–609, 1999.

[4] W. W. Yu, L. Qu, W. Guo, and X. Peng, "Experimental determination of the extinction coefficient of cdte, cdse, and cds nanocrystals," *Chemistry of Materials*, vol. 15, no. 14, pp. 2854–2860, 2003.

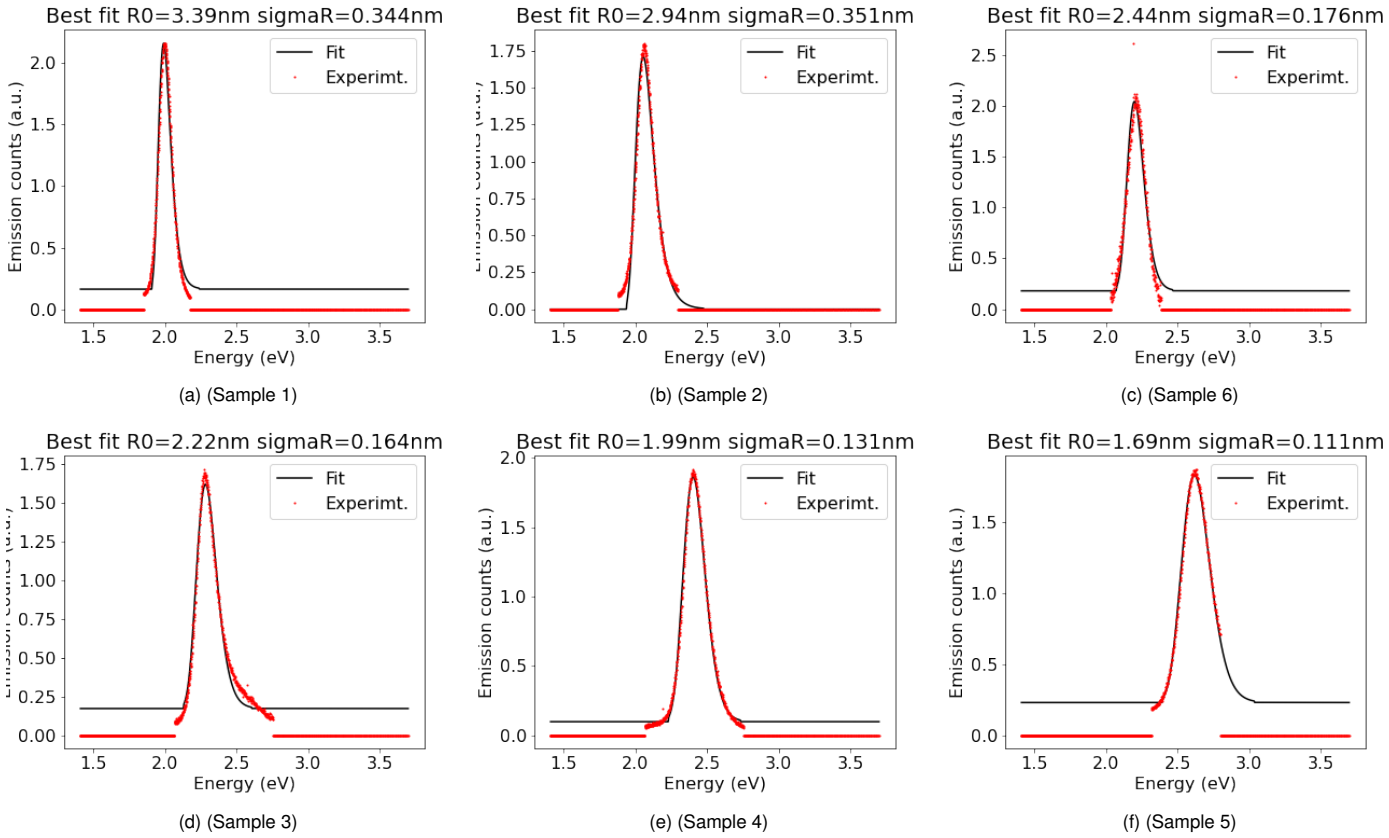

(a) (Sample 1) (b) (Sample 2) (c) (Sample 6)

(d) (Sample 3) (e) (Sample 4) (f) (Sample 5)

Figure 4: Selected experimental data in red and theoretical fit using the finite quantum potential well model in black.

[5] L. E. Brus, "Electron–electron and electron-hole interactions in small semiconductor crystallites: The size dependence of the lowest excited electronic state," *The Journal of chemical physics*, vol. 80, no. 9, pp. 4403–4409, 1984.

[6] J. Marin, R. Riera, and S. Cruz, "Confinement of excitons in spherical quantum dots," *Journal of Physics: Condensed Matter*, vol. 10, no. 6, p. 1349, 1998.

[7] D. L. Ferreira, J. Sousa, R. Maronesi, J. Bettini, M. Schiavon, A. V. Teixeira, and A. G. Silva, "Size-dependent bandgap and particle size distribution of colloidal semiconductor nanocrystals," *The Journal of chemical physics*, vol. 147, no. 15, p. 154102, 2017.

[8] P. e. a. Virtanen and SciPy 1.0 Contributors, "SciPy 1.0: Fundamental Algorithms for Scientific Computing in Python," *Nature Methods*, vol. 17, pp. 261–272, 2020.

[9] "Github repository with the material generated for the physics at the nanoscale practice of group 13." https://github.com/Oiangu9/Physics_at_the_Nanoscale_Reports.

[10] B. O. Dabbousi, J. Rodriguez-Viejo, F. V. Mikulec, J. R. Heine, H. Mattoussi, R. Ober, K. F. Jensen, and M. G. Bawendi, "(cdse)zns coreshell quantum dots: synthesis and characterization of a size series of highly luminescent nanocrystallites," *The Journal of Physical Chemistry B*, vol. 101, no. 46, pp. 9463–9475, 1997.